NASA CR-166,407

NASA CONTRACTOR REPORT 166407

Accelerated Fatigue Durability of a High Performance Composite

A. Rotem

CONTRACT NAS2– 10228
September 1982

NASA

NASA CONTRACTOR REPORT 166407

Accelerated Fatigue Durability of a High Performance Composite

Dr. Assa Rotem
Advanced Research and Applications Corporation
Sunnyvale, California 94086

Prepared for
Ames Research Center
under Contract NAS2-10228

National Aeronautics and
Space Administration

Ames Research Center
Moffett Field, California 94035

INTRODUCTION

The fatigue durability of a material depends upon the variety of conditions in which the material is required to perform. It is especially so for high-performance composites, made of graphite fibers in an epoxy matrix. Conditions like load sequence, frequency, temperature, etc., tend to change the fatigue durability. The research discussed in this report was concerned with the influence of temperature on the tension-tension fatigue behavior of a laminated graphite-epoxy composite, and with the possibility of using certain temperature phenomena to extend the time or cycles scale of fatigue.

In a previous study,[1] it was found that the fatigue behavior of graphite-epoxy angle-ply laminates can be characterized by the principal failure strengths of the lamina, the fatigue functions and the temperature shifting factors. Thus, a fatigue failure criterion for matrix failure of some lamina (within a laminate) is given by

$$\frac{p^{\sigma_T^c}}{\sigma_T^u}^2 + \frac{p^{\tau^c}}{\tau^u}^2 \geq 1 \tag{1}$$

where $p^{\sigma_T^c}$ and p^{τ^c} are the cyclic transverse tension and inplane shear, respectively, of some lamina, p, and σ_T^u and τ^u are the principal fatigue strengths. These fatigue strengths can be expressed by the static strengths, σ_T^s and τ^s, and the fatigue functions, f_T and f_τ, as follows:

$$\sigma_T^u = \sigma_T^s f_T (R_1 N_1 n_1 T) \tag{2}$$

$$\tau^u = \tau^s f_\tau (R_1 N_1 n_1 T)$$

The fatigue functions depend on the loading ratio, R, number of cycles, N, speed of cycling, n, and the temperature, T. Since both the statis strength and the fatigue function depend on temperature, it is

possible to shift both from one temperature level to another by means of shifting factors, i.e., a_i^s for the static strength and $a_i(T)$ for the fatigue function. The S-N curve of any principal strength can be presented by a master curve at a reference temperature level, T_o. The S-N curve at any other temperature can be determined by substituting the relevant shifting factor. This is expressed as follows:

$$\sigma_i^u(T) = \sigma_i^{(s)}(T_o)\, f_i\, (a_i^s, a^i(T), N, T_o) \tag{3}$$

In a general laminate, there are five principal strengths, A, T, τ, Z, d, which are active in three failure modes. A is the tension in the fiber direction which results in fiber failure. T is the tension transverse to fiber direction and τ is the inplane shear -- both cause inplane failure. Z is the tension between layers (interlaminar) and d is the interlaminar shear -- both cause interlaminar failure.

The prediction of the fatigue durability of a laminate involves the calculation of the principal stresses acting in each lamina and between laminae due to the external loading. Substituting these principal stresses into the three fatigue failure criteria to find the shortest number of cycles which would cause failure for a specific mode. For simple laminates, this procedure was found successful[1] and gave good results. More complicated laminates, like symmetrical-balanced laminates, need further analysis to establish failure mechanisms, because of the dependence of the principal stresses on the external loading through the moduli of the composite material. Since the matrix is a polymeric resin, the moduli of the composite are viscoelastic. The principal stresses can change with time as a result of the redistribution of the external loads. The fatigue durability is also changed due to the change in the magnitude of the principal stresses. This report deals with symmetrical-balanced laminates, their behavior in fatigue at different temperatures, and the possibility of temperature shifting and predicting the fatigue durability of these complex laminates.

MATERIALS AND PROCEDURES

Graphite epoxy (T300/5208) prepreg tapes were used to fabricate panels having a symmetrical-balanced structure.* Each panel consisted of eight layers with an average fiber volume fraction of 65%. Graphite cloth composite (5208 resin) was used as end-tabs and glued to the panel before it was cut into specimens. Specimen dimensions are as shown in Figure 1. The graphite cloth end-tabs were required because all other types of tabs (glass fiber, aluminum) did not hold under the combined conditions of fatigue and elevated temperature. Specimens with the following construction were used in this program: angle-ply $\pm 30^{\circ}$ and $\pm 45^{\circ}$ for characterization of the viscoelastic relations; symmetrical-balanced laminates $\left[0^{\circ},30^{\circ},0^{\circ}\right]_s$, $\left[0^{\circ},\pm45^{\circ},0^{\circ}\right]_s$, $\left[0^{\circ},\pm45^{\circ},90^{\circ}\right]_s$ and $\left[0^{\circ},\pm30^{\circ},90^{\circ}\right]_s$, for verifying perdictions of fatigue durability and failure mechanisms, based on experimentally-determined parameters and proposed theory; symmetrical-balanced laminates, $\left[0^{\circ},\pm45^{\circ},90^{\circ}\right]_s$ and $\left[90^{\circ},\pm45^{\circ},0^{\circ}\right]_s$, for analysis of the different failure mechanisms in fatigue due to the different construction of the laminate.

All types of specimens were tested at three temperatures: $22^{\circ}C$ ($72^{\circ}F$), $74^{\circ}C$ ($165^{\circ}F$), and $115^{\circ}C$ ($237^{\circ}F$). Tests were performed on a hydraulic, servo-controlled testing machine at a frequency of 10 cycles per second and a loading ratio of R = 0.1 (minimum tension amplitude to maximum tension amplitude). Specimens were soaked at the testing temperature for at least one hour (without loading) prior to testing.

---

*The fabrication of specimens was done by Lockheed Missiles and Space Co., Sunnyvale, California.

RESULTS AND DISCUSSION

Complex Modulus Measurements

Loading of a symmetrical-balanced laminate along the symmetric axis results in a stress in each lamina in the direction given by

$$ {}_p\sigma_x^c = E_x^c \left({}_pQ_{xx} - {}_1V_{xy}\, {}_pQ_{xy} \right) \tag{4} $$

where E_x^c is the strain in all of the laminae, ${}_pQ_{xx}$ and ${}_pQ_{xy}$ are the moduli of the individual lamina under consideration, and ${}_1V_{xy}$ is the Poisson's ratio of the whole laminate. The principal stresses in each lamina are given by the relations

$$ \begin{aligned} {}_p\sigma_A^c &= {}_pk_{xx}\, {}_p\sigma_x^c \\ {}_p\sigma_T^c &= {}_pk_{yy}\, {}_p\sigma_x^c \\ {}_p\tau^c &= {}_pk_{yx}\, {}_p\sigma_x^c \end{aligned} \tag{5} $$

where ${}_pk_{ij}$ are a function of the angle, θ, which the load axis makes with the fiber direction and the orthotropic moduli.[2] Out of the four moduli, only the inplane shear, G_A, shows heavy dependence on time. (Although E_T is also matrix dominated, it shows only a small time dependence.) Therefore, our analysis will include the time-dependent behavior of the shear modulus G_A.

When loaded under oscillating load, the shear stress-shear strain behavior can take one of two forms shown in Figure 1, depending upon whether the stress amplitude or the strain amplitude is kept constant. Two things are changed with the number of cycles: (1) the peak value either of strain or stress, and (2) the slope of the oscillating stress-strain relationship. These values are important in order to calculate the existing stress field in the laminate. The best way to describe this behavior is by the secant modulus of the mean stress, G_A^M, and the complex modulus, G_A^*. Both moduli are stress dependent because of the

nonlinearity. The secant modulus, G_A^M, is the ratio between the mean stress level and the mean strain level at a particular number of cycles (or time). The complex modulus, G_A^*, is the ratio between the stress amplitude and the strain amplitude at a particular number of cycles (or time) and for a particular mean stress level.

Measurements were performed on a $\pm 45^o$ angle-ply laminate with two extensometers -- longitudinal and transverse. From these results, the shear moduli were determined. The shear complex modulus is shown in Figure 2 for three different temperatures as a function of the peak stress amplitude, where the mean stress level and the amplitude are combined. As can be seen, both the stress level and temperature change the modulus significantly. Instead of the mean shear secant modulus, the peak shear secant modulus, G_A^C, will be used, because it simplifies the calculations. The peak shear secant modulus, G_A^C, is the ratio of the maximum shear stress in a cycle to the maximum shear strain in the cycle. The values of the secant modulus for three different temperatures as a function of the stress amplitude are shown in Figure 3.

In many cases when a general laminate is subjected to a constant stress amplitude cycle, each lamina within the laminate will be subjected to an almost constant strain amplitude cycle. Therefore, it is simpler to use the shear moduli as a function of the strain level. The peak shear secant modulus, G_A^C, as a function of the shear strain amplitude for three different temperatures is shown in Figure 4.

In addition to the stress dependence, the shear modulus will also depend on the number of cycles (or time). Under stress amplitude loading, the matrix creeps and influences the shear secant modulus. For example, the creep of the shear secant modulus under a load amplitude of 44.7 MPa at 74^oC is shown in Figure 5. The shear complex modulus is less affected by stress amplitude cycling and shows a significant change only when failure is approached. However, a change of up to 10% is noticeable as early as half the fatigue life. On the other hand, the secant modulus changes significantly after the first one thousand cycles. It is important to note that at a slightly lower stress amplitude of 37.4 MPa, there is no change in the complex modulus and the material does not fail. In view of

these creep properties, the mechanism of failure of multidirectional laminate appears to be as follows: constant stress amplitude cycling on the laminate is introduced on each lamina as strain amplitude cycling, with the amplitude changed as the stiffness of the whole laminate changes. The stiffness of symmetrical-balanced laminates, with sufficient fibers in the load direction, does not change much with cycling. In such a case, each lamina is under almost constant strain amplitude, when the laminate is under constant stress amplitude. The stress amplitude on the inclined laminae is relaxed with number of cycles. The results of constant strain amplitude tests imposed on $\pm 45^{\circ}$ angle-ply laminates are shown in Figure 6 for different strain levels and temperatures. It is seen that all the laminates failed after some relaxation period. The strain levels were lower than the strain failure level of a unidirectional lamina. The relaxation of the stress amplitude of a $\pm 30^{\circ}$ angle-ply is shown in Figure 7, where the strain amplitude level is about half the failure strain of a unidirectional laminate. The $\pm 30^{\circ}$ laminate did not fail under these conditions but only relaxed about 25%.

When an angle-ply is incorporated with a unidirectional lamina to form a symmetrical-balanced laminate of the form $\left[0^{\circ},\pm\theta^{\circ},0^{\circ}\right]_s$, some of the load relaxed from the $\pm\theta^{\circ}$ laminae is transferred to the 0° laminae. Results of fatigue strength tests of a $\left[0^{\circ},\pm 45^{\circ},0^{\circ}\right]_s$ laminate at two temperatures are shown in Figure 8, with a S-N line indicating the fatigue failure if all the load was carried by the 0° laminae. It is hard to distinguish between the behavior at the two temperatures, because the strength contribution of the $\pm 45^{\circ}$ laminae is very small. A comparison of these results with the fatigue strengths of $\left[0^{\circ},\pm 60^{\circ},0^{\circ}\right]_s$, $\left[0^{\circ},\pm 75^{\circ},0^{\circ}\right]_s$ and $\left[0^{\circ},\pm 90^{\circ},0^{\circ}\right]_s$ shows that the $\left[0^{\circ},\pm 45^{\circ},0^{\circ}\right]_s$ laminate is somewhat stronger, as seen in Figure 9. It can be concluded that laminates of the form $\left[0^{\circ},\pm\theta^{\circ},0^{\circ}\right]_s$ with $\theta \geq 45^{\circ}$ are dominated by the fiber fatigue strength, and their behavior is as if the fibers of the 0° laminae carry all of the load.

When the angle $\theta < 45^{\circ}$, the inclined laminae are contributing to the fatigue strength, and their failure leads to the failure of the whole laminate, as can be seen in Figure 10 for the $\left[0^{\circ},\pm 30^{\circ},0^{\circ}\right]_s$ laminate.

The fiber failure mode of this laminate is much higher than the observed data, i.e., if the $\pm$ 30° laminae were carrying the load to the point where the fibers of these laminae fail. On the other hand, if the load was carried solely by the 0° fibers, the fatigue strength would have been much lower than the observed results.

For the case when the inclined laminae dominate the fatigue failure, shifting of the S-N curve due to temperature is possible. It has been shown in Reference 2 that an "artificial" static strength shifting factor, $a_i^{s'}$, can be used and expressed as:

$$1 - a_i^{s'} = \left(\frac{T_o \left[{}^{o}K \right]}{T \left[K \right]} \right)^{\frac{1}{2}} \tag{6}$$

where the "artificial" static strength is the extrapolated fatigue strength at one cycle. It was determined[2] that the fatigue function could be expressed in the form

$$f_i = a_i(T) \left(\frac{1}{a_i(T)} - b_i \log N \right) - a_i^{s'} \tag{7}$$

For the T300/5208 laminates, $a_i(T)$ was found not to be a function of temperature. Therefore, the shifting of the S-N curve due to temperature only occurs by the shifting of the artificial static strength through the shifting factor, $a_i^{s'}$. The values of the fatigue functions were found to be

$$\left.\begin{aligned} f_\tau &= 1 - 0.0735 \log N - \left(1 - \left(\frac{T_o \left[{}^{o}K \right]}{T \left[{}^{o}K \right]} \right)^{\frac{1}{2}} \right) \\ &= \left(\frac{T_o \left[{}^{o}K \right]}{T \left[{}^{o}K \right]} \right)^{\frac{1}{2}} - 0.0735 \log N \end{aligned} \right\} \tag{8}$$

$$f_T = \left(\frac{T_o \left[{}^{o}K \right]}{T \left[{}^{o}K \right]} \right)^{\frac{1}{2}} - 0.080 \log N$$

The predicted S-N curves are shown in Figure 10 for two temperature levels, and are in good agreement with the experimental results.

Failure Mechanism

The mechanism of failure and the influence of stacking sequence were examined on the laminates of $\left[0^{o},\pm45^{o},90^{o}\right]_{s}$ and $\left[90^{o},\pm45^{o},0^{o}\right]_{s}$. The predicted mechanism of failure for both laminates is the $\pm45^{o}$ laminae first crack at a strain level of 4.9×10^{-3}. This causes a relief of the constraint by the 0^{o} laminae. $\pm 45^{o}$ laminae act as an angle-ply laminate, which is stronger and start to fail only at a strain of 11.5×10^{-3}. Therefore, the 90^{o} laminae fail first at a strain of 6.1×10^{-3}, the 0^{o} laminae fail second at strain of 11×10^{-3} and is followed immediately by failure of the $\pm 45^{o}$ laminae. The "artificial" static strength will be the strength of the fibers plus the stress in the $\pm 45^{o}$ laminae at this strain.

$$_{\ell}\sigma_{xx}^{s'} = \tfrac{1}{4}\,(1510) + \tfrac{1}{2}\,(12.8 \times 10^{3} \times 11 \times 10^{-3}) = 448 \text{ MPa}$$

The fatigue strength will be dominated by the fatigue function of the fibers. To calculate the fatigue strength of the laminate, we must consider the relaxation of the stress in the $\pm 45^{o}$ laminae. Using the data in Figure 6 and the fatigue function of the fibers,[2]

$$f_{A} = 1 - 0.033 \log N \tag{9}$$

we can calculate the S-N curve for the laminate.

For example

$$N = 10^{3}: \quad \sigma_{A}^{u} = 1510\,(1 - 0.033 \log 10^{3}) = 1360 \text{ MPa}$$

$$_{\ell}\sigma_{x}^{c} = \tfrac{1}{4}\,(1360) + \tfrac{1}{2}\left(\frac{1360}{136 \times 10^{3}}\ 12.8 \times 10^{3} \times 0.6\right) = 378 \text{ MPa}$$

The predicted S-N curve and the experimental results are shown in Figures 11 and 12. Also shown is the S-N curve for the case where all of the load was carried by the 0° laminae. It is seen that there is some contribution to the strength of the laminate by the $\pm 45^{\circ}$ laminae, and that the lay-up sequence has no influence on the strength of the laminate. This conclusion is based on the predicted failure mechanism, as the laminae act in parallel, so that interlaminar failure will not change the stress field in the laminate. This conclusion was verified by the experimental results (as seen in Figures 11 and 12).

To demonstrate the relaxation of the stress on the $\pm 45^{\circ}$ laminae, constant strain amplitude tests were performed on a $\left[90^{\circ},\pm 45^{\circ},0^{\circ}\right]_s$ laminate at a temperature of $114^{\circ}C$ and on a $\left[0^{\circ},\pm 45^{\circ},90^{\circ}\right]_s$ laminate at a temperature of $25^{\circ}C$. The results of these tests are shown in Figure 13 and demonstrate the relaxation of the stresses in the $\pm 45^{\circ}$ laminae. The high-temperature test results fall below the room-temperature results for the same strain level because of the lower moduli.

Even though the strength of both laminates is the same, the fracture process, especially in fatigue, is different. During static failure, only few cracks appear prior to final fracture. But in fatigue, the 90° laminae continue to form cracks as cycling continues. As a result, these laminae disintegrate. For the $\left[90^{\circ},\pm 45^{\circ},0^{\circ}\right]_s$ laminate, the 90° laminae disintegrated and peeled off, as seen in Figure 14. The remaining laminae form a symmetrical-balanced laminate of $\left[\pm 45^{\circ},0^{\circ}\right]_s$. In contrast, the disintegration of the 90° laminae of the $\left[0^{\circ},\pm 45^{\circ},90^{\circ}\right]_s$ laminate forms two separate unbalanced laminates of $\left[0^{\circ},\pm 45^{\circ}\right]$, Figure 14, which are loaded in parallel. But, because of the delamination stresses between the 0° lamina and the 45° lamina in both types of laminates, the constraint on the $\pm 45^{\circ}$ lamina is relieved and we end up in both types of laminates with 0° laminae and a $\pm 45^{\circ}$ angle-ply laminate loaded in parallel. Therefore, the static strength and the fatigue behavior of both types of laminate are equivalent.

The failure mechanism prediction of the laminate $\left[0^{\circ},\pm 30^{\circ},90^{\circ}\right]_s$ is as follows. The 90° laminae fails first and no longer contributes to the strength of the laminate. At a higher strain level, the $\pm 30^{\circ}$ laminae

are released from the constraint by the 0° laminae due to high interlaminar shear, and act as a $\pm 30^{\circ}$ angle-ply laminate. Parallel loading of the $\pm 30^{\circ}$ and the 0° laminae cause failure of the $\pm 30^{\circ}$ laminae by inplane shear. Subsequently, the 0° laminae cannot carry the extra load, and they fail catastrophically. This mechanism of failure implies that fatigue failure is governed by the inplane shear cracking of the $\pm 30^{\circ}$ laminae.

The experimental results and the predicted S-N curves (dashed lines) are shown in Figure 15 for two temperatures. However, since the 90° laminae fail first, there was an extra load on the $\pm 30^{\circ}$ laminae, which results in a more rapid failure or a stiffer fatigue function. The corrected S-N curves due to prefailure of the 90° laminae and due to the creep of the $\pm 30^{\circ}$ laminae are shown as solid lines in Figure 15. The temperature effect was found to obey the same law and the shifting factor was found to agree with the experimental results.

SUMMARY

The fatigue behavior of multidirectional graphite-epoxy laminates was analyzed theoretically and experimentally in an effort to establish an accelerated testing methodology. Analysis of the failure mechanism in fatigue of the laminates led to the determination of the failure mode governing fracture. The nonlinear, cyclic-dependent shear modulus was used to calculate the changing stress field in the laminate during the fatigue loading. Fatigue tests were performed at three different temperatures: 25°C, 74°C, and 114°C. The prediction of the S-N curves was made based on the "artificial" static strength at a reference temperature and the fatigue functions associated with them. The prediction of an S-N curve at other temperatures was performed using shifting factors determined for the specific failure mode.

For multidirectional laminates, different S-N curves at different temperatures could be predicted using these shifting factors. Different S-N curves at different temperatures occur only when the fatigue failure mode is matrix dominated. It was found that whenever the fatigue failure mode is fiber dominated, temperature, over the range investigated, had no influence on the fatigue life.

These results permit the prediction of long-time, low-temperature fatigue behavior from data obtained in short-time, high-temperature testing, for laminates governed by a matrix failure mode.

PUBLICATION

A paper entitled "Fatigue Behavior of Graphite-Epoxy Laminates at Elevated Temperatures" was presented at the ASTM conference held in San Francisco on May 22-23, 1979.

The material in the paper was based in part on this research. The paper is enclosed as an Appendix.

REFERENCES

1. Assa Rotem and Howard G. Nelson, "A Temperature Dependent Fatigue Failure Criterion for Graphite/Epoxy Laminates," NASA Technical Memorandum 78538, October 1978.

2. Assa Rotem and Howard G. Nelson, "Fatigue Behavior of Graphite-Epoxy Laminates at Elevated Temperatures," NASA Technical Memorandum, September 1979.

LIST OF CAPTIONS

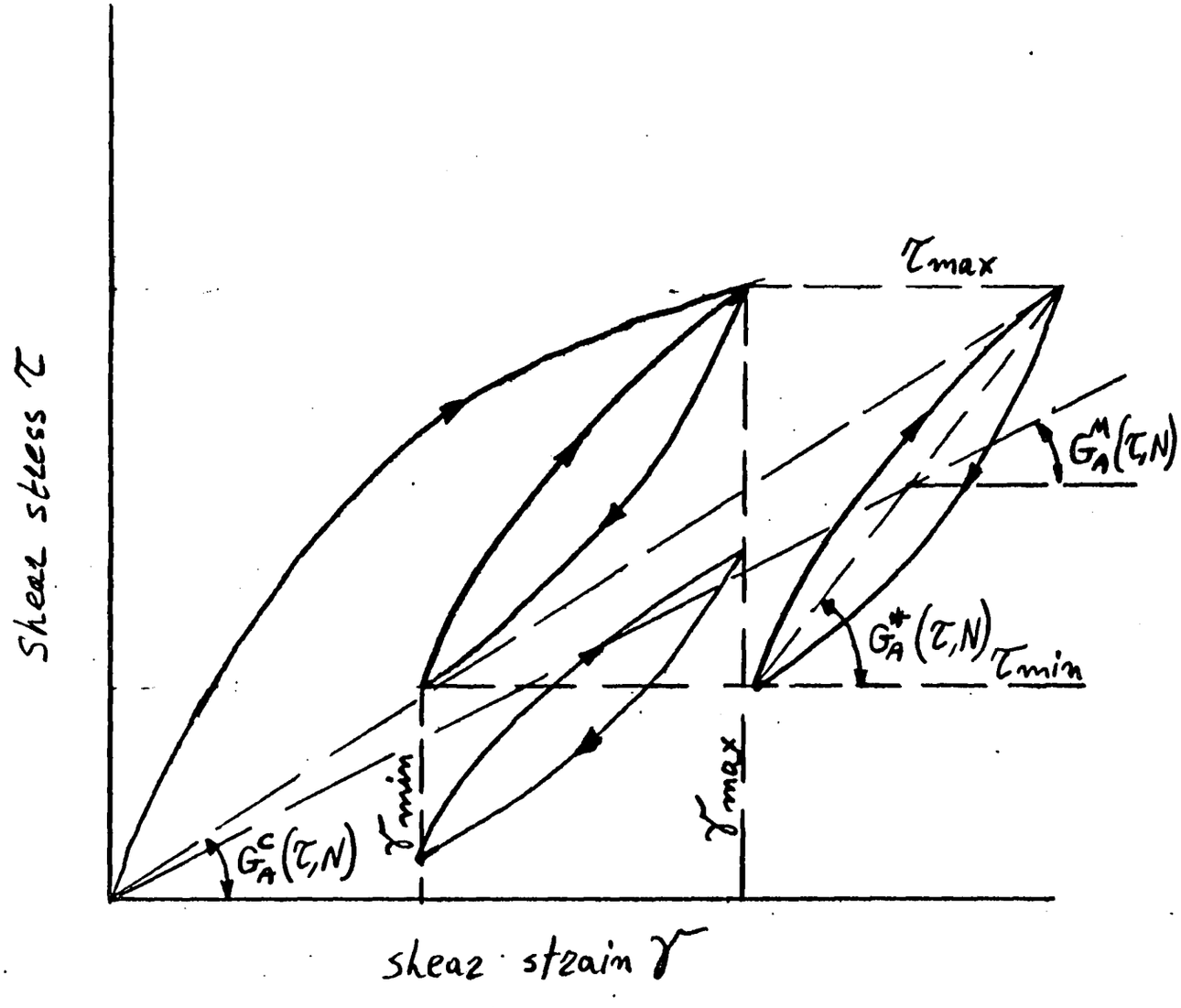
Shear stress τ
τmax
τmin
γmin
γmax
$G_A^c(\tau,N)$
$G_A^M(\tau,N)$
$G_A^*(\tau,N)$
shear strain γ

Figure 1

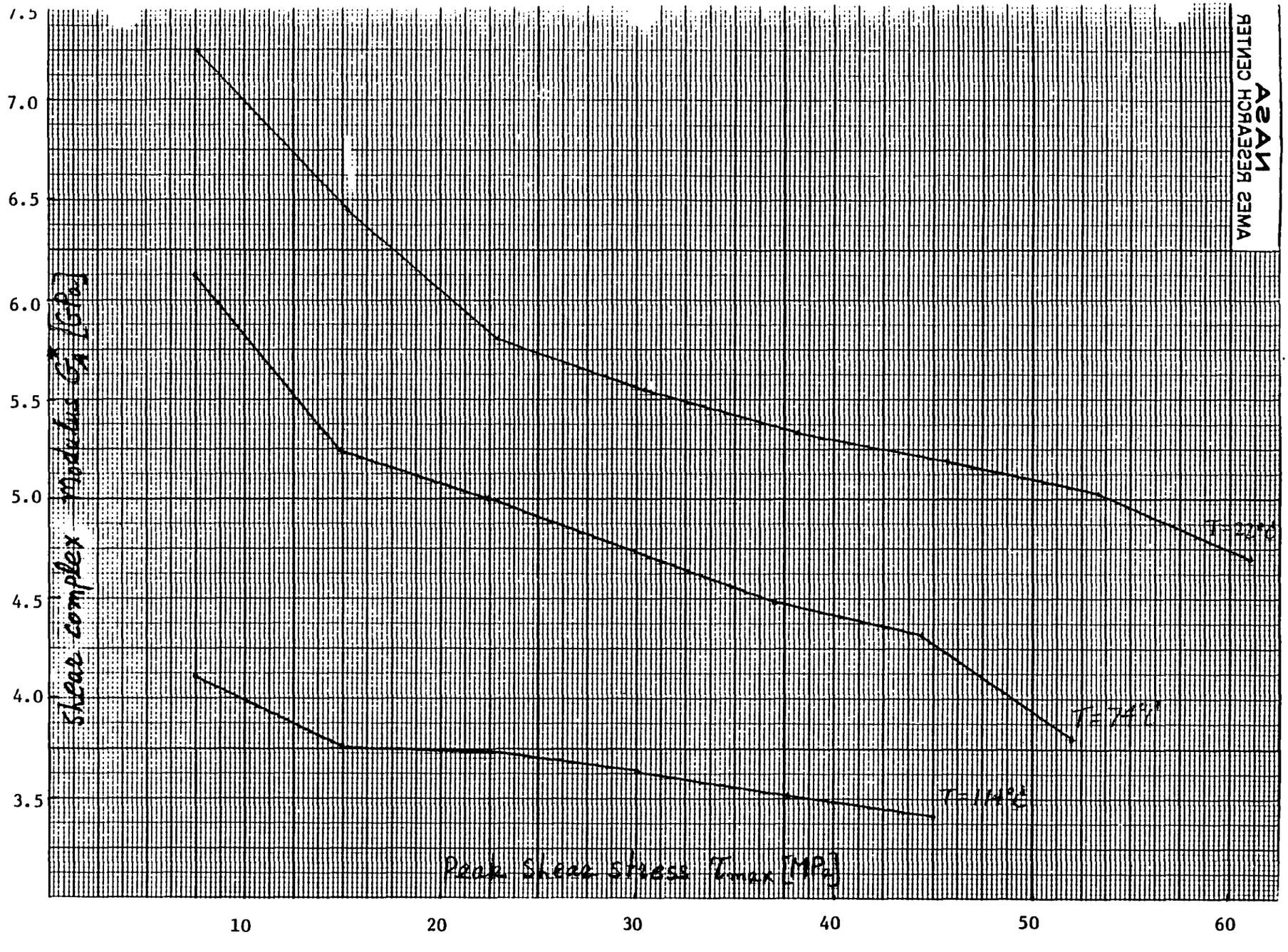
NASA
AMES RESEARCH CENTER
7.5
7.0
6.5
6.0
5.5
5.0
4.5
4.0
3.5
Shear complex modulus G* [GPa]
Peak Shear Stress τ_{max} [MPa]
10
20
30
40
50
60
T = 24°C
T = 114°C

Figure 2

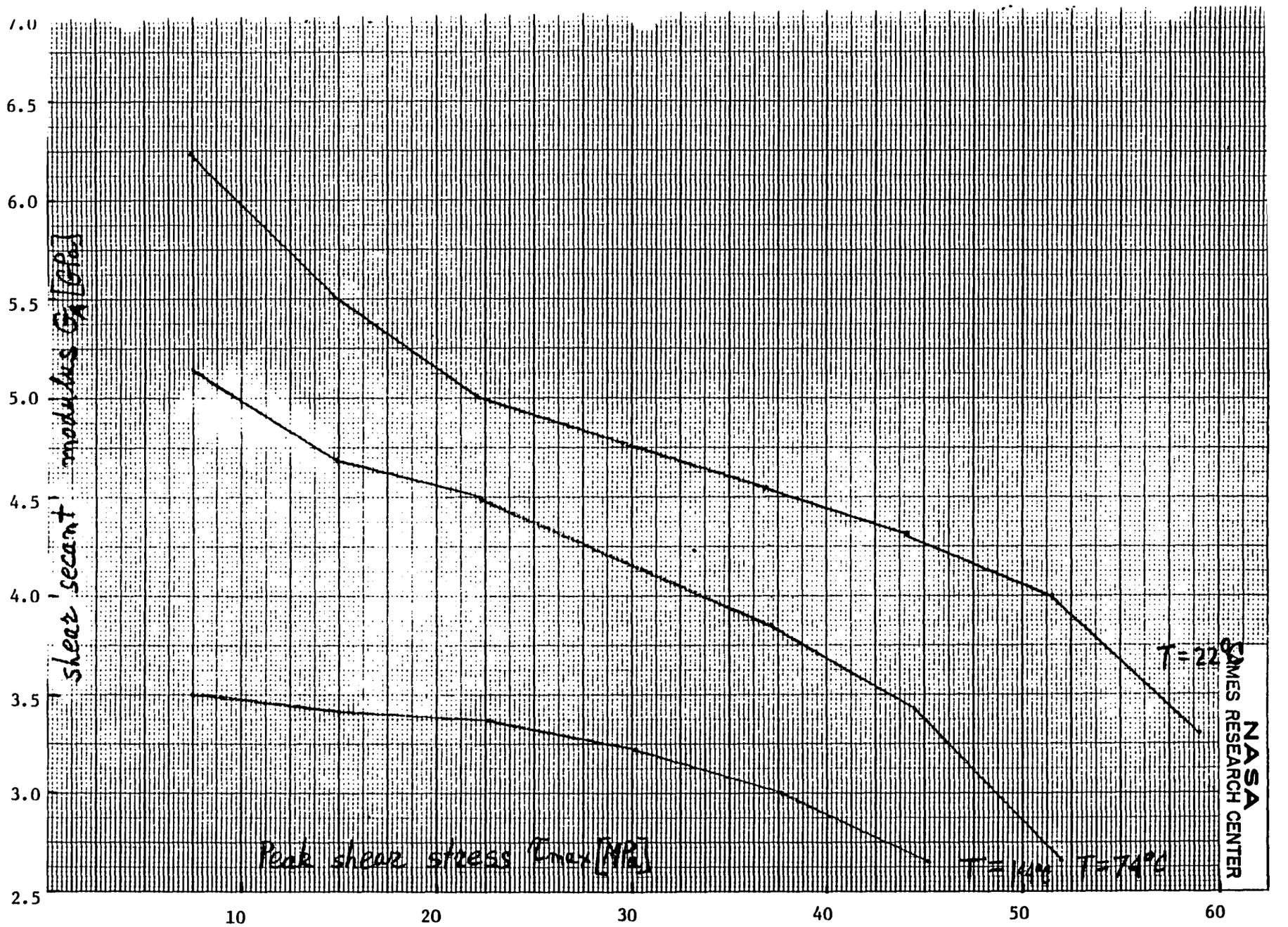
7.0
6.5
6.0
5.5
5.0
4.5
4.0
3.5
3.0
2.5
10
20
30
40
50
60
shear secant modulus G [GPa]
Peak shear stress τmax [MPa]
T = 24°C
T = 144°C
T = 74°C
NASA
AMES RESEARCH CENTER

Figure 3

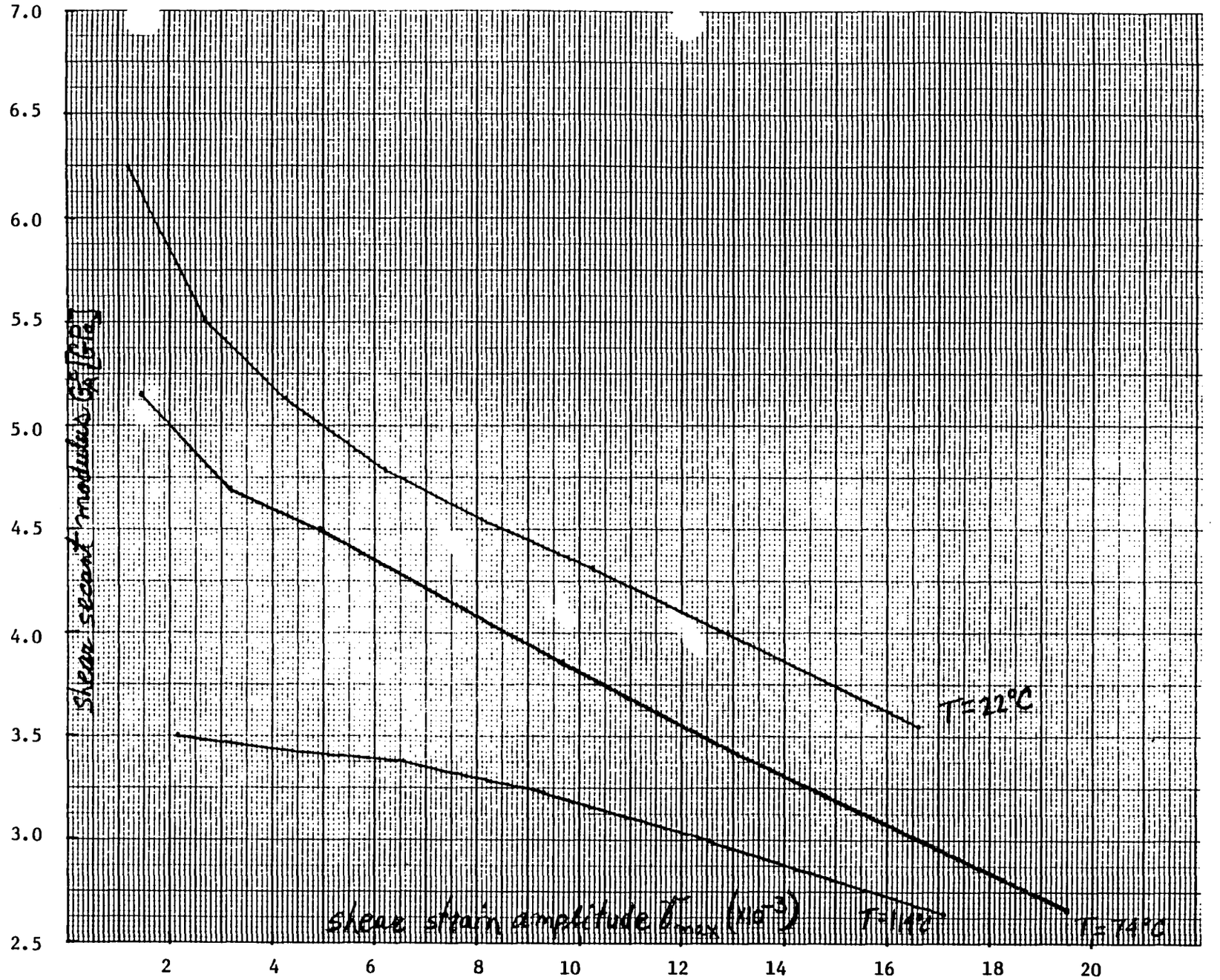

Figure 4

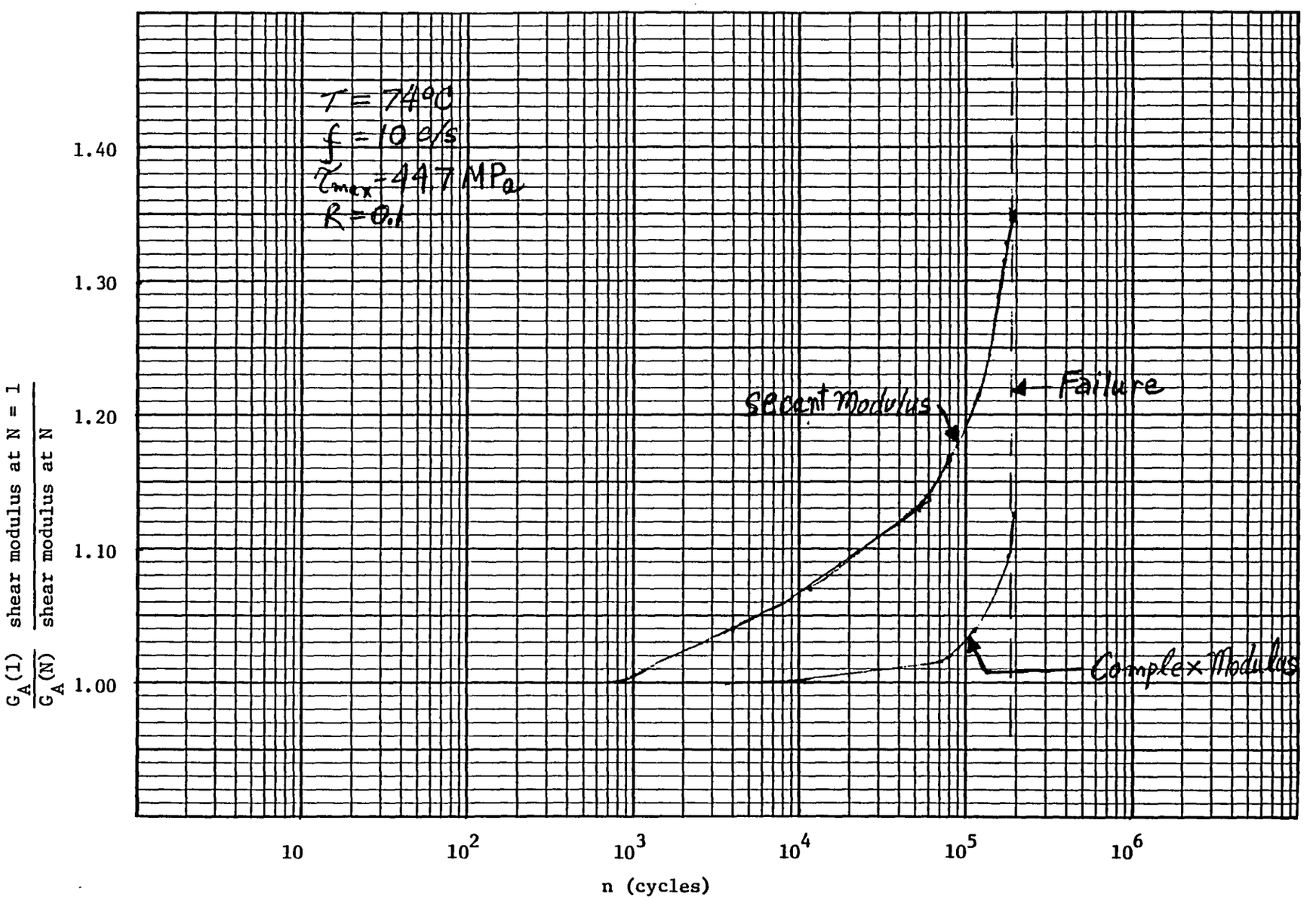
T = 74°C
f = 10 c/s
τmax = 4.47 MPa
R = 0.1
Secant Modulus
Failure
Complex Modulus
1.40
1.30
1.20
1.10
1.00
GA(1) / GA(N) shear modulus at N = 1 / shear modulus at N
10
10^2
10^3
10^4
10^5
10^6
n (cycles)

Figure 5

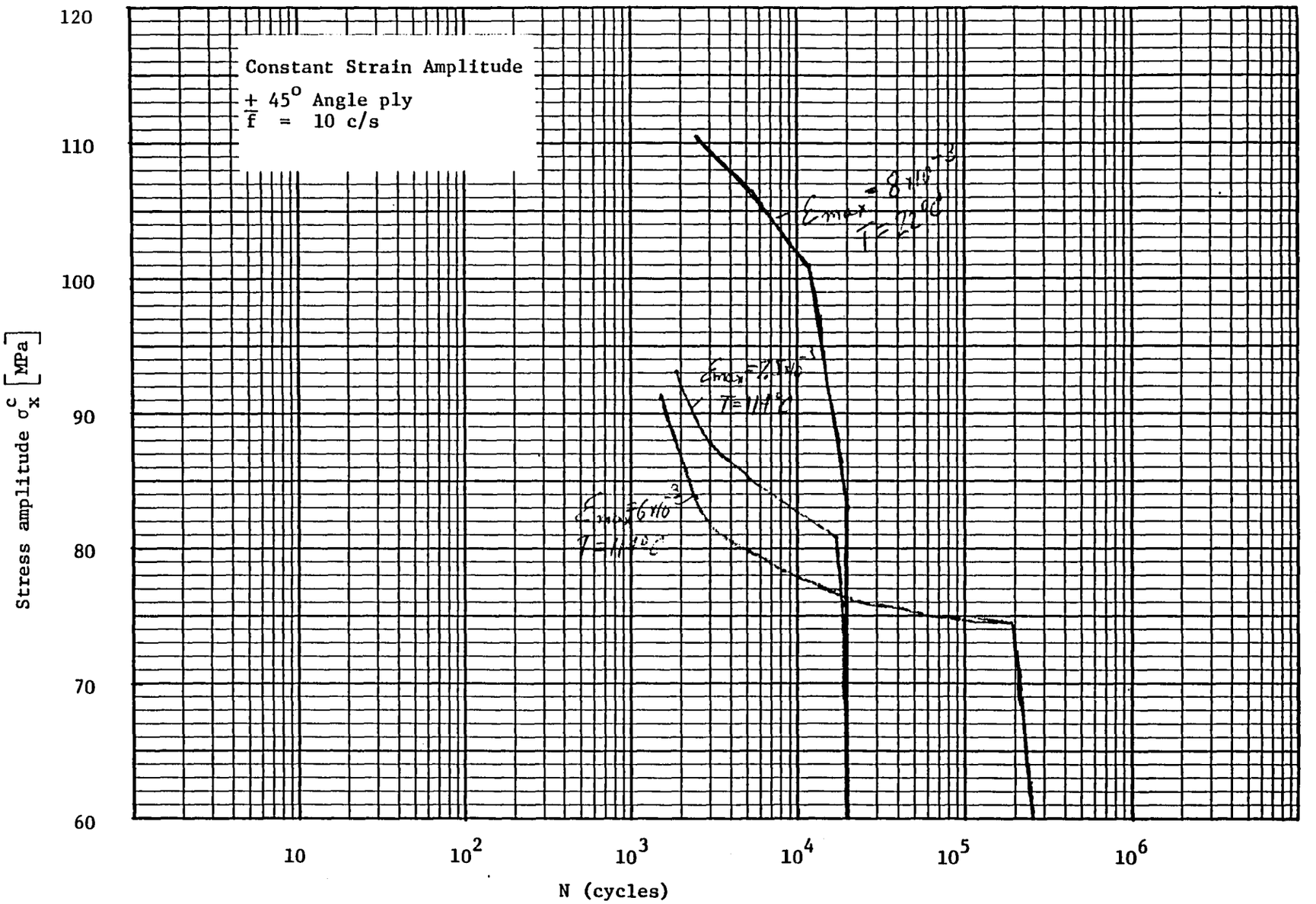
Constant Strain Amplitude
± 45° Angle ply
f = 10 c/s
120
110
100
90
80
70
60
Stress amplitude σ_x^c [MPa]
10
10^2
10^3
10^4
10^5
10^6
N (cycles)

Figure 6

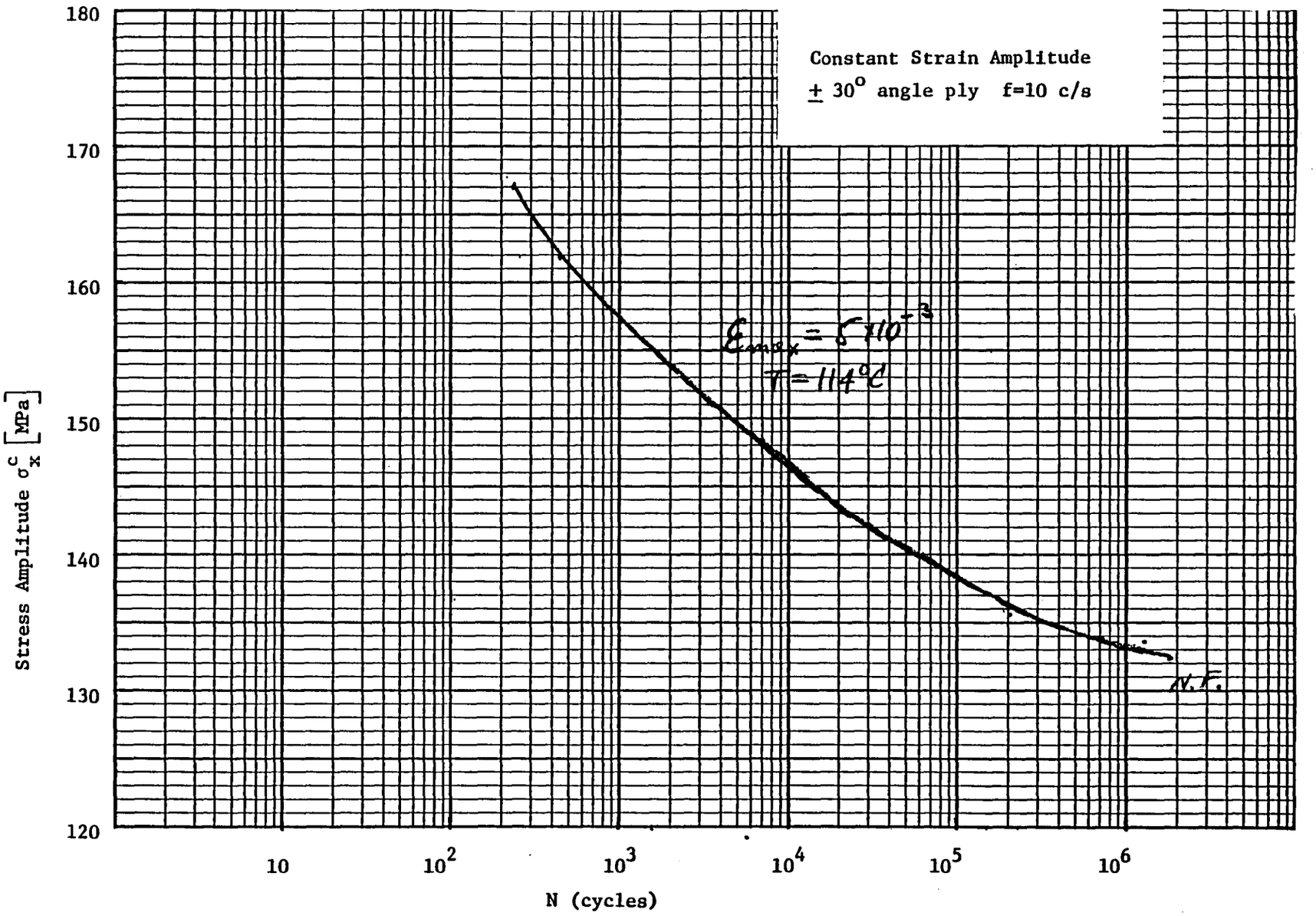
Constant Strain Amplitude
± 30° angle ply f=10 c/s
$\varepsilon_{max} = 5 \cdot 10^{-3}$
T = 114°C
N.F.
Stress Amplitude σ_x^c [MPa]
180
170
160
150
140
130
120
10
10^2
10^3
10^4
10^5
10^6
N (cycles)

Figure 7

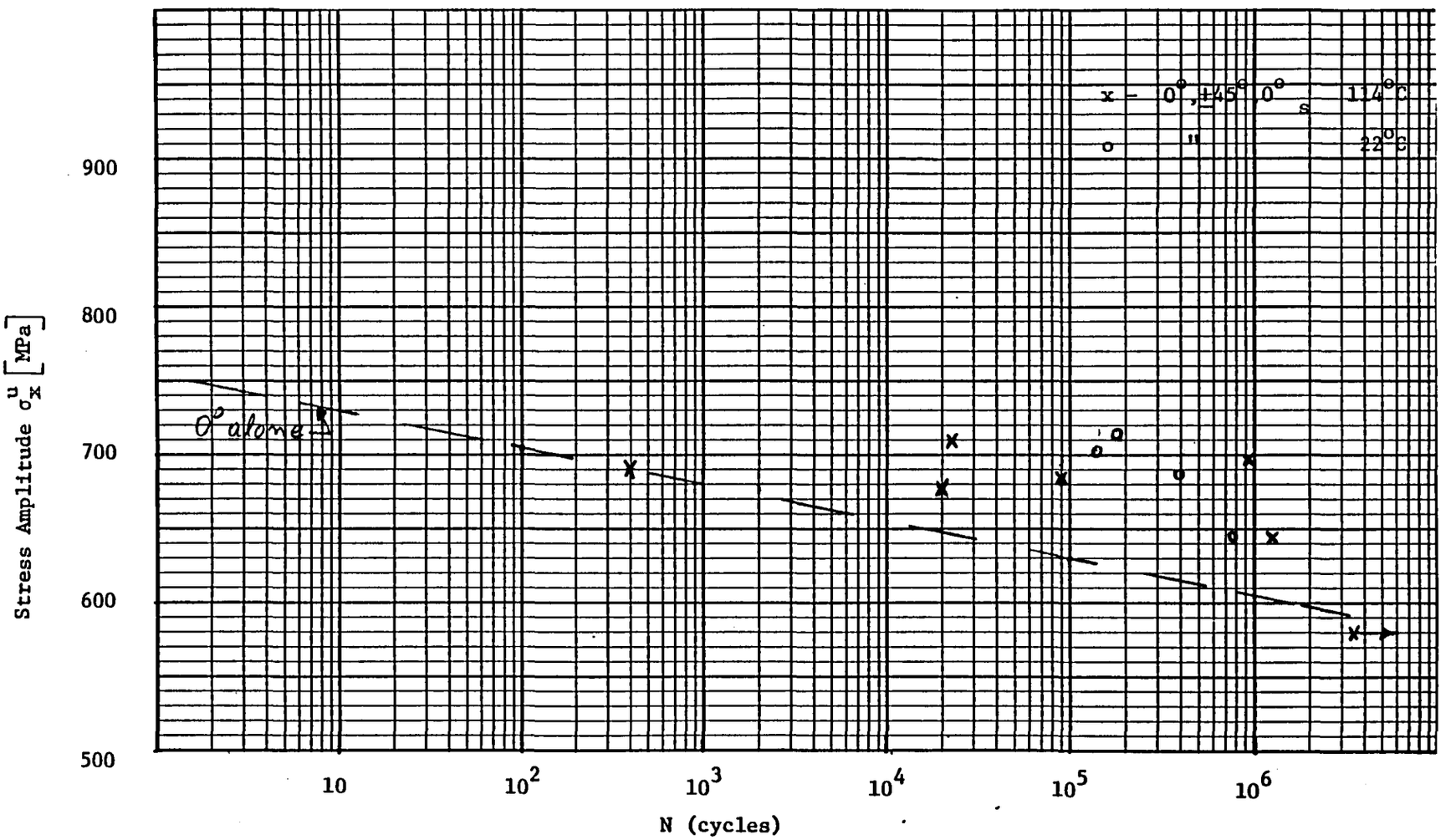
x = 0°,±45°,0°s 114°C
" 22°C
0° alone
900
800
700
600
500
Stress Amplitude σ_x^u [MPa]
10
10^2
10^3
10^4
10^5
10^6
N (cycles)

Figure 8

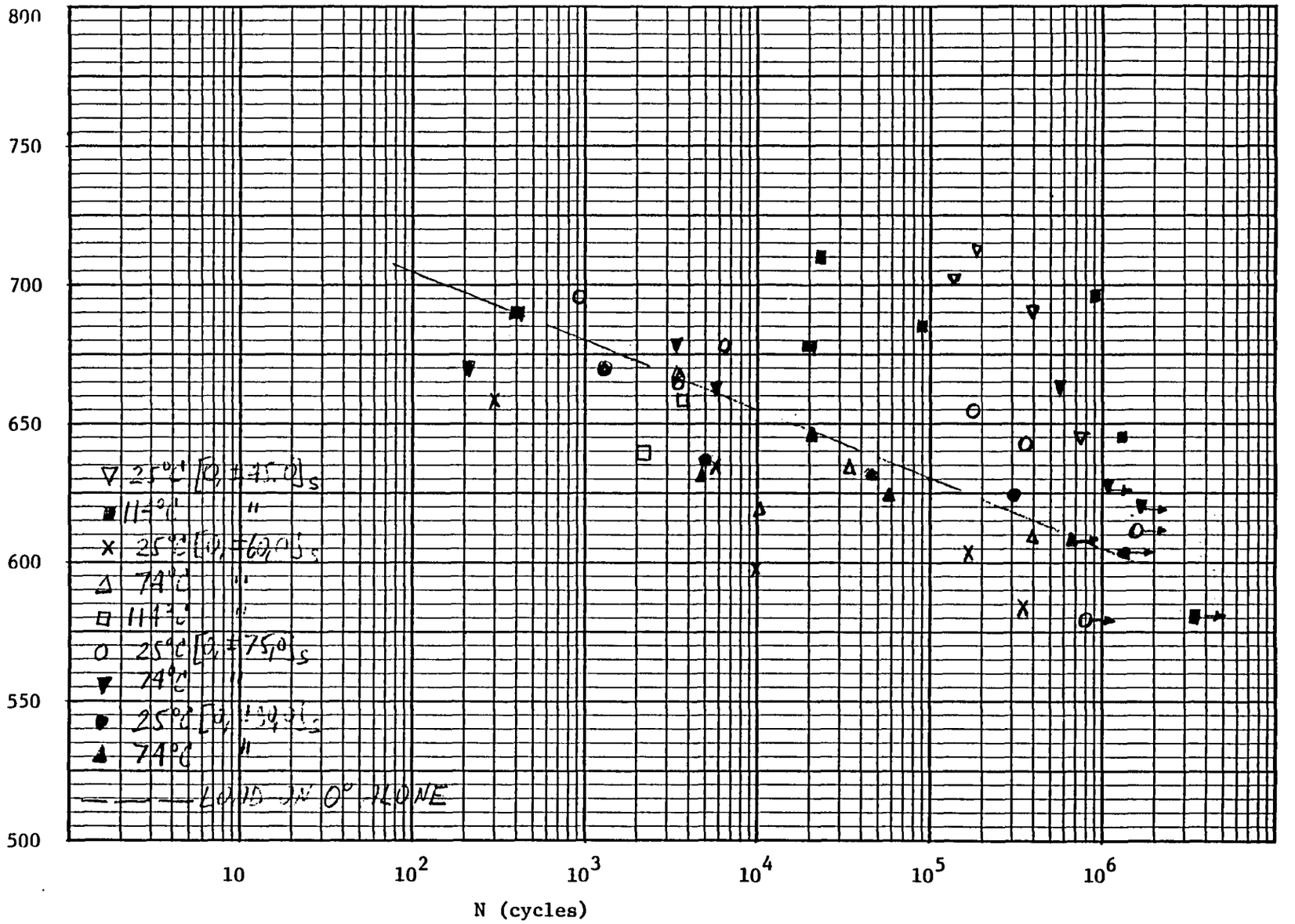
800
750
700
650
600
550
500
Stress Amplitude σ_x^u [MPa]
10
10^2
10^3
10^4
10^5
10^6
N (cycles)
25°C [θ = ±45.0]s
114°C "
25°C [θ = ±60.0]s
74°C "
114°C "
25°C [θ = ±75.0]s
74°C "
25°C [θ = ±54.7]s
74°C "
LOADS IN 0° PLANE

Figure 9

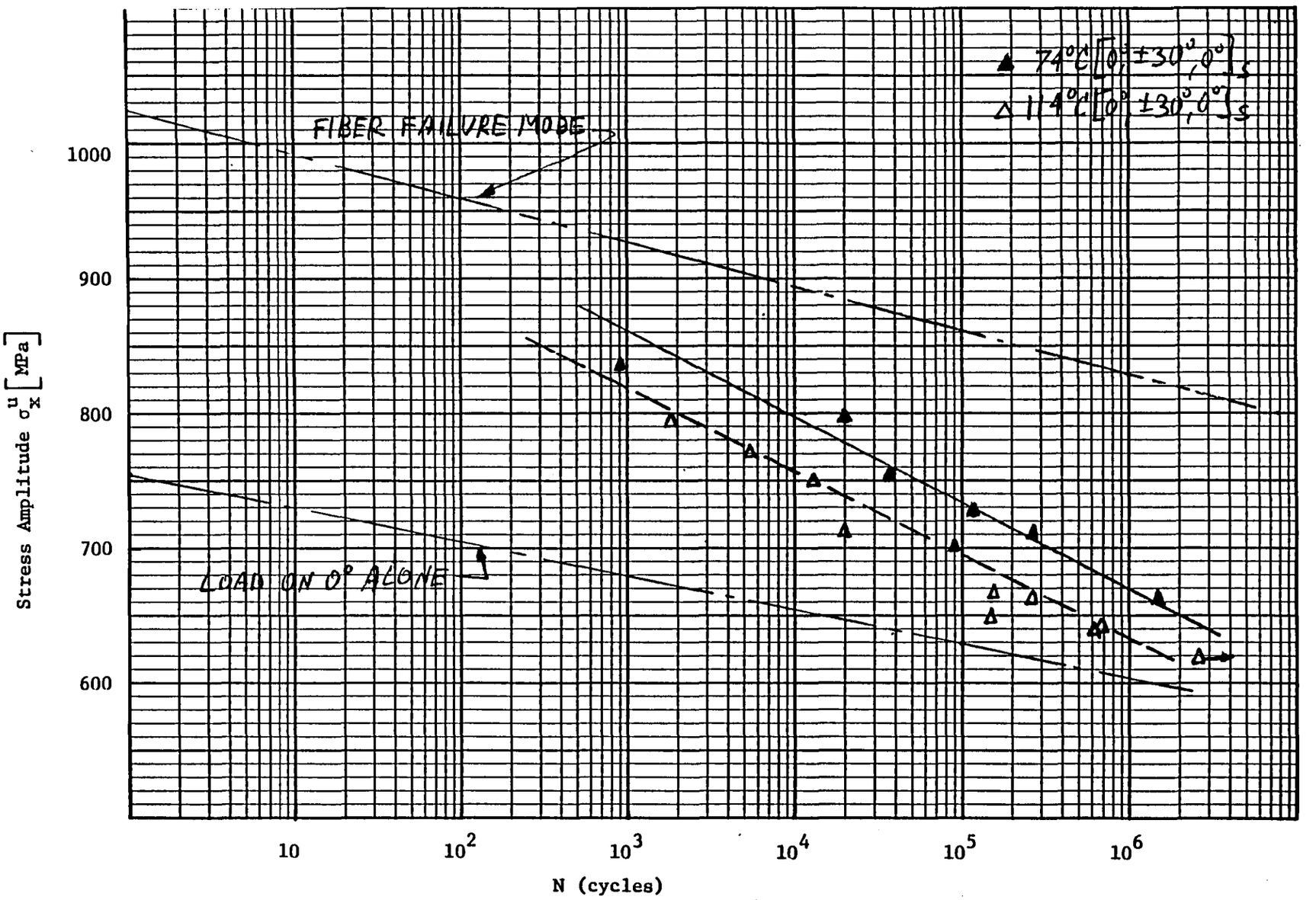
▲ 74°C [0, ±30°, 0°]s
△ 114°C [0°, ±30°, 0°]s
FIBER FAILURE MODE
LOAD ON 0° ALONE
1000
900
800
700
600
Stress Amplitude σ_x^u [MPa]
10
10^2
10^3
10^4
10^5
10^6
N (cycles)

Figure 10

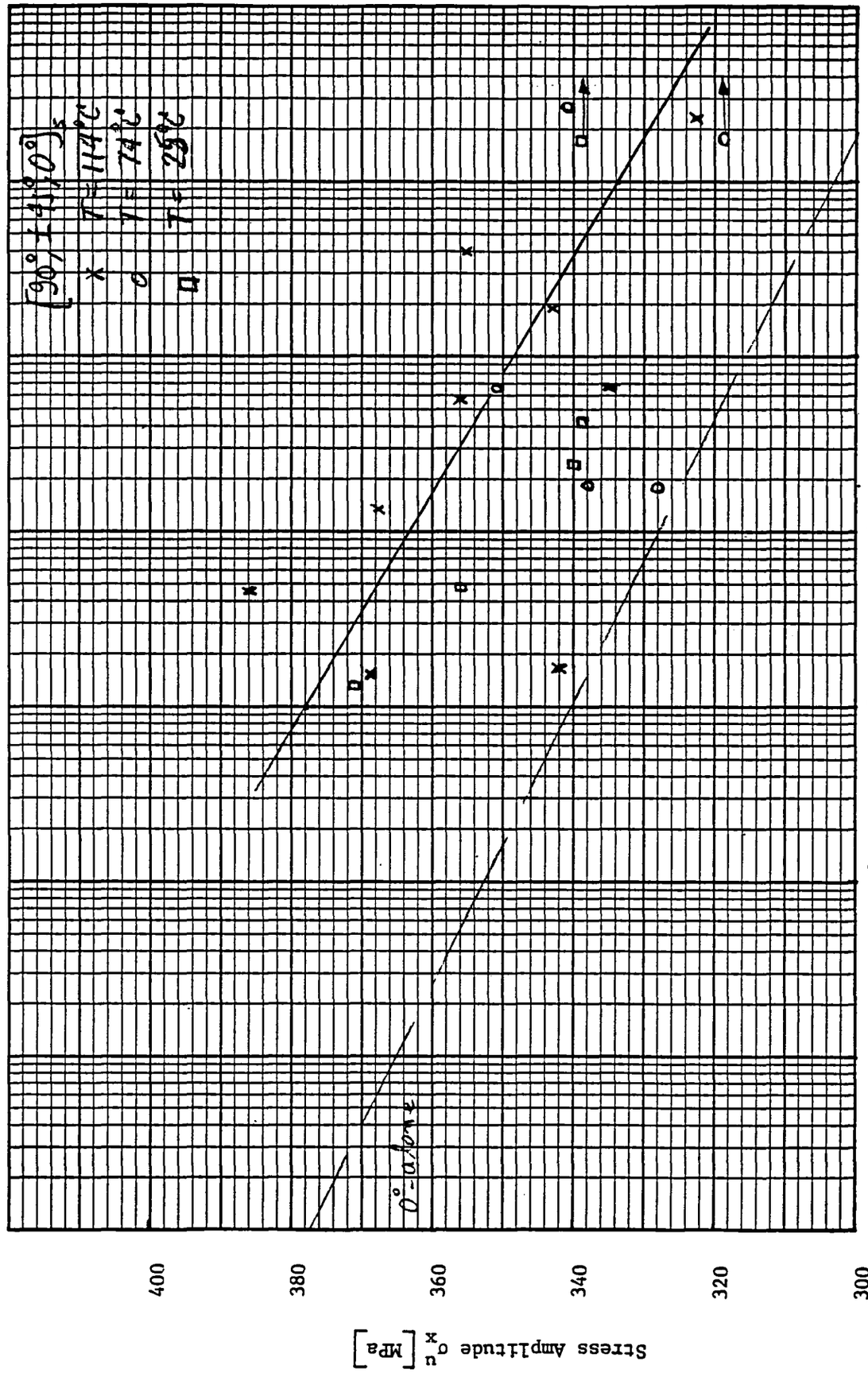
Stress Amplitude σ_x^u [MPa]
400
380
360
340
320
300
10
10^2
10^3
10^4
10^5
10^6
N (cycles)
$[90°, \pm 45°, 0°]_s$
x T = 114°C
o T = 74°C
□ T = 25°C
0°-direction

Figure 11

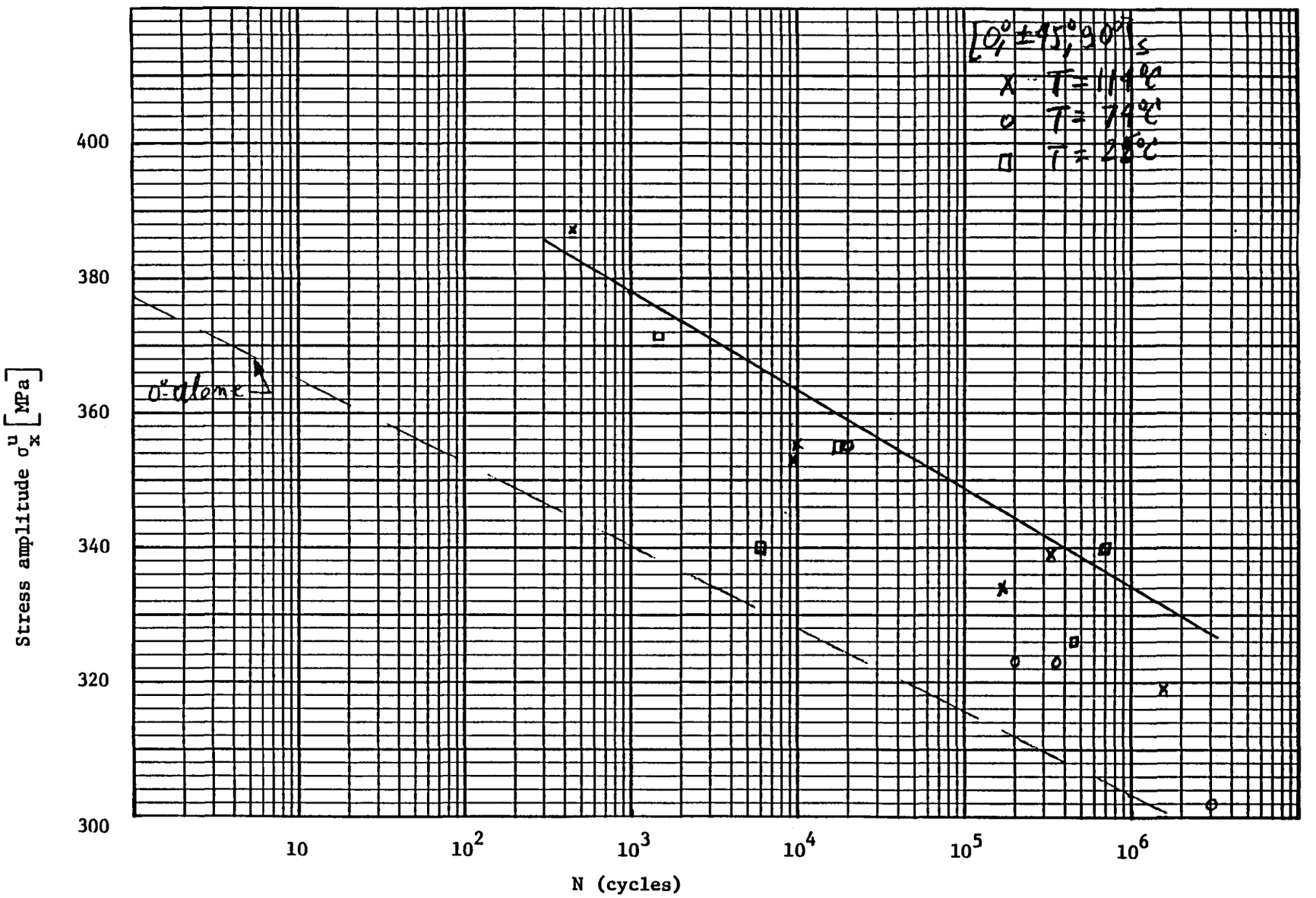
Stress amplitude σ_x^u [MPa]
400
380
360
340
320
300
10
10^2
10^3
10^4
10^5
10^6
N (cycles)
$[0°/\pm45°/90°]_s$
x T = 114 °C
o T = 74 °C
□ T = 28 °C
0°-akorn

Figure 12

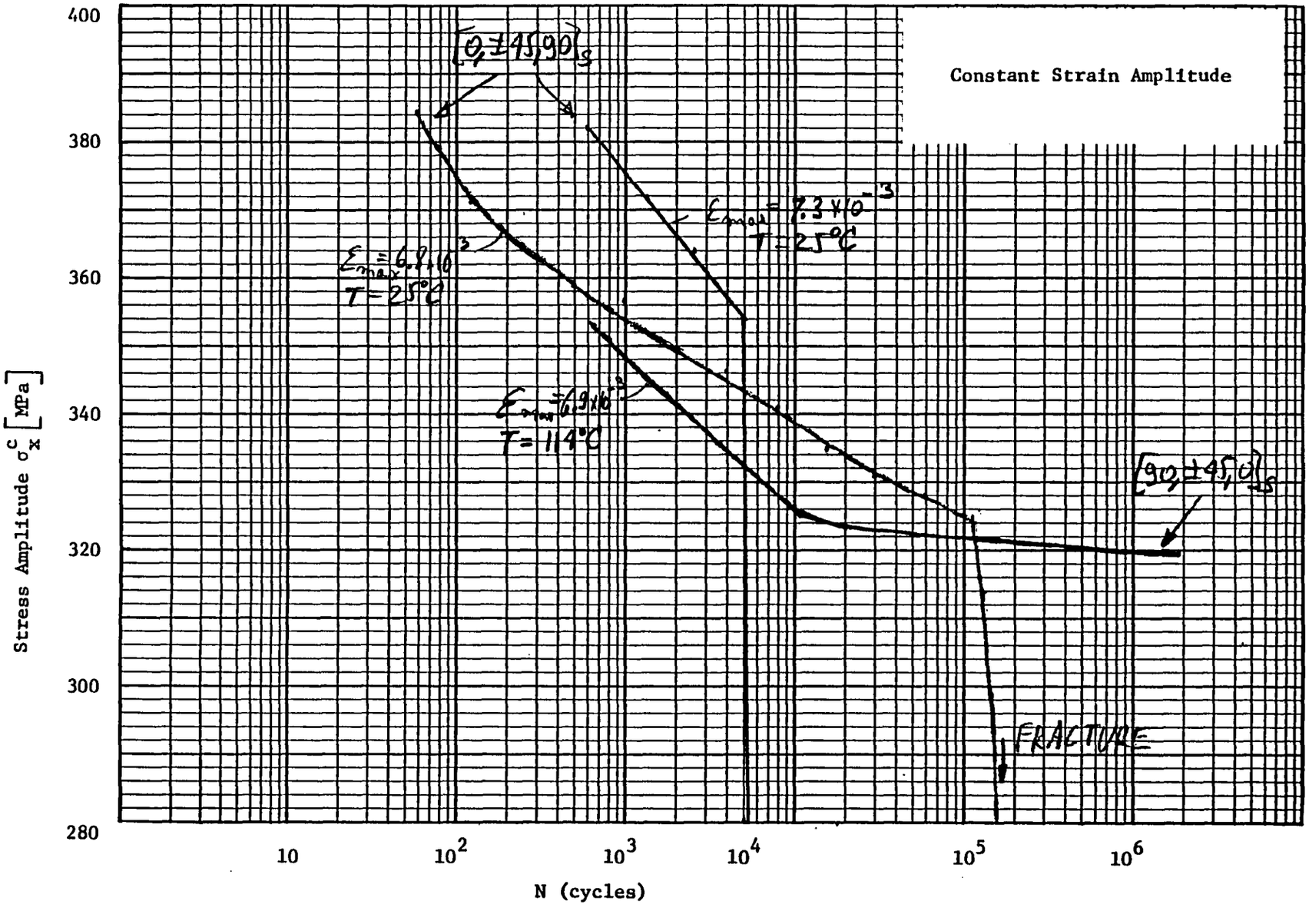
Constant Strain Amplitude
[0,±45,90]s
$\varepsilon_{max} = 7.3 \times 10^{-3}$
T = 25°C
$\varepsilon_{max} = 6.8 \times 10^{-3}$
T = 25°C
$\varepsilon_{max} = 6.9 \times 10^{-3}$
T = 114°C
[90,±45,0]s
FRACTURE
Stress Amplitude σ_x^c [MPa]
400
380
360
340
320
300
280
10
10^2
10^3
10^4
10^5
10^6
N (cycles)

Figure 13

$[90^{\circ}, \pm 45^{\circ}, 0^{\circ}]_s$

$[0^{\circ}, \pm 45^{\circ}, 90^{\circ}]_s$

Figure 14

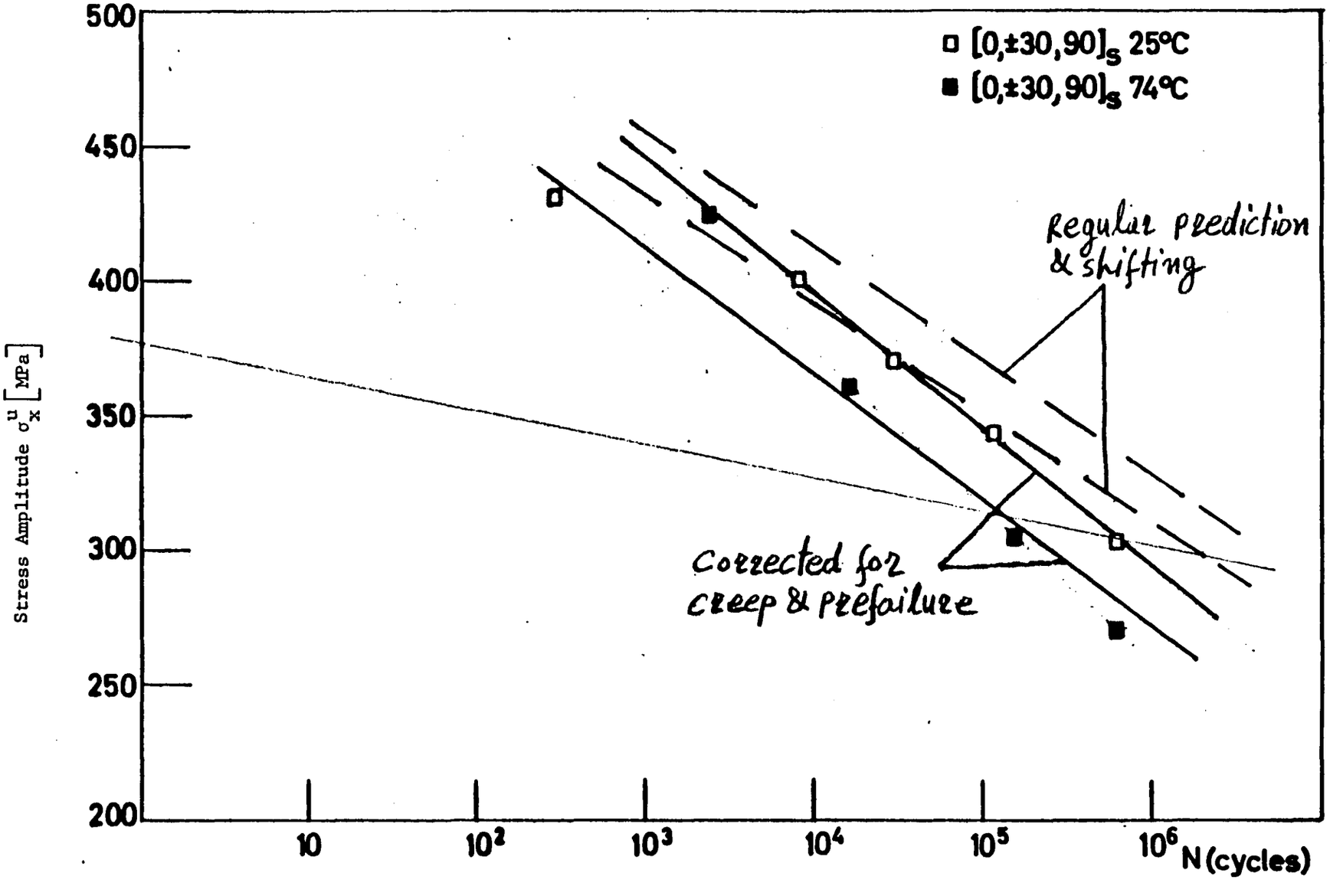
500
450
400
350
300
250
200
10
10^2
10^3
10^4
10^5
10^6
N (cycles)
Stress Amplitude σ_x^u [MPa]
□ $[0,\pm30,90]_S$ 25°C
■ $[0,\pm30,90]_S$ 74°C
Regular prediction & shifting
Corrected for creep & prefailure

Figure 15

1. Report No.	2. Government Accession No.	3. Recipient's Catalog No.
CR-166407		

4. Title and Subtitle	5. Report Date
ACCELERATED FATIGUE DURABILITY OF A HIGH PERFORMANCE COMPOSITE	October 1979
	6. Performing Organization Code
7. Author(s)	8. Performing Organization Report No.
Assa Rotem	
9. Performing Organization Name and Address	10. Work Unit No.
Advanced Research and Applications Corporation 1223 E. Arques Avenue Sunnyvale, CA 94086	11. Contract or Grant No. NAS2-10228
12. Sponsoring Agency Name and Address	13. Type of Report and Period Covered Contractor Report Final Report
National Aeronautics and Space Administration Washington, DC 20546	14. Sponsoring Agency Code

15. Supplementary Notes

Point of Contact: Dr. Howard G. Nelson, 230-4, NASA-Ames Research Center, Moffett Field, CA 94035, (415) 965-6137, FTS 448-6137

16. Abstract

The fatigue behavior of multidirectional graphite-epoxy laminates was analyzed theoretically and experimentally in an effort to establish an accelerated testing methodology. Analysis of the failure mechanism in fatigue of the laminates led to the determination of the failure mode governing fracture. The nonlinear, cyclic-dependent shear modulus was used to calculate the changing stress field in the laminate during the fatigue loading. Fatigue tests were performed at three different temperatures: 25°C, 74°C, and 114°C. The prediction of the S-N curves was made based on the "artificial" static strength at a reference temperature and the fatigue functions associated with them. The prediction of an S-N curve at other temperatures was performed using shifting factors determined for the specific failure mode.

For multidirectional laminates, different S-N curves at different temperatures could be predicted using these shifting factors. Different S-N curves at different temperatures occur only when the fatigue failure mode is matrix dominated. It was found that whenever the fatigue failure mode is fiber dominated, temperature, over the range investigated, had no influence on the fatigue life.

These results permit the prediction of long-time, low-temperature fatigue behavior from data obtained in short-time, high-temperature testing, for laminates governed by a matrix failure mode.

17. Key Words (Suggested by Author(s))	18. Distribution Statement
accelerated testing, failure modes, fatigue life perdiction, tension-tension fatigue.	Unlimited STAR Category - 24

19. Security Classif. (of this report)	20. Security Classif. (of this page)	21. No. of Pages	22. Price*
Unclassified	Unclassified	32	

*For sale by the National Technical Information Service, Springfield, Virginia 22161

End of Document